A Linear MMSE Receiver for SWIPT-enabled Wireless Networks

Yuan Guo, Christodoulos Skouroumounis, and Ioannis Krikidis
IRIDA Research Centre for Communication Technologies
Department of Electrical and Computer Engineering, University of Cyprus
Email: {yguo0001, cskour03, krikidis}@ucy.ac.cy

***Abstract*—In this paper, we investigate the performance of a linear minimum mean square error (MMSE) receiver in the context of simultaneous wireless information and power transfer (SWIPT)-enabled cellular networks. Specifically, the multi-antenna user equipments (UEs) are equipped with a linear MMSE receiver and employ either the time switching (TS), the power splitting (PS) or the antenna switching (AS) schemes to achieve the SWIPT capability, while a non-linear energy harvesting (EH) model is considered. The performance achieved by a linear MMSE receiver in the considered network deployment is evaluated in terms of multiple key performance metrics, e.g. information decoding (ID) and EH coverage probabilities, average spectral efficiency and average harvested energy. By leveraging tools from stochastic geometry, we establish an analytical and tractable framework to evaluate the aforementioned performance metrics, of which the analytical expressions are derived. Our results reveal that the ID performance achieved by the MMSE receiver outperforms that of the conventional maximum ratio combining, leading to an enhanced EH performance, for a given ID reliability constraint. Moreover, by using a linear MMSE receiver, PS scheme offers the best SWIPT performance compared to TS and AS schemes.**

***Index Terms*—SWIPT, MMSE receiver, stochastic geometry.**

I. Introduction

Motivated by the pressing demand on the sustainable energy supply and ultra-reliable connectivity of the emerging massive Internet of Things (mIoT) in the sixth generation networks, simultaneous wireless information and power transfer (SWIPT) become ever more attractive [1]. Specifically, SWIPT technology enables diverse range of mobile devices to extract both information and energy from the received radio-frequency (RF) signals [2]. Moreover, the concept of mIoT leads to fearful multi-user interference, motivating the employment of advanced receiver architectures for mitigating the interference and enhancing the performance of end-user devices.

The concept of SWIPT is referred to splitting the received RF signals in two parts; one part is used for information transfer and another part is used for power transfer. The partitioning of RF signals is performed either in the time, the power, or the space domain, via the employment of the time switching (TS), power splitting (PS) or antenna switching (AS) schemes, respectively [2], [3]. Throughout the literature, the potential benefits of SWIPT have been widely studied [2]–[5]. The authors in [3] investigate the performance of a SWIPT-enabled multiple-input multiple-output (MIMO) wireless broadcast system in the context of several receiver architectures for TS, PS and AS schemes, presenting the fundamental trade-off between data and energy transfer. The authors in [4] propose a stochastic geometry-based framework to investigate SWIPT-enabled MIMO systems under the TS and the PS schemes, where the optimal partitioning parameters to achieve best joint information decoding (ID) and energy harvesting (EH) performance is demonstrated. Moreover, the concept of SWIPT in intelligent reflecting surface (IRS)-assisted cellular networks is investigated in [5], highlighting that the IRSs can facilitate in compensating the high RF signal attenuation over long distance and thereby establish effective energy harvesting/charging zones for hotspot areas in their proximity.

Due to the dense deployment of mIoT applications, the unprecedented increment of the multi-user interference becomes the dominant factor jeopardizing the network performance. Motivated by this, the employment of advanced receiver architectures such as the minimum mean square error (MMSE) and the maximum ratio combining (MRC) are proposed to enhance the end-user performance. Under the special scenario where the interference can be treated as white noise, the MRC is an optimal receiver that achieves the highest output signal-to-noise ratio [6]. However, the consideration of multi-user interference as white noise is a suboptimal assumption, especially in large-scale networks where the interference observed at different UEs' antennas is spatially correlated [7]. By taking into consideration the interference impact, the MMSE receiver is indicated to achieve a maximum output signal-to-interference-plus-noise ratio (SINR) [8], [9]. The authors in [8] derive the exact distribution for the output SINR of an ideal MMSE receiver, where multiple interferers and Rayleigh fading channel are considered. This work is further extended in [9], by considering a random number of interferers, illustrating the optimal network density that offers the highest network spatial throughput. Although the performance of the MMSE receiver has been extensively studied, the co-design of SWIPT and MMSE is overlooked from the literature.

In this paper, we study the SWIPT performance for multi-antenna UEs in terms of a linear MMSE receiver. In particular,

This work has received funding from the European Research Council (ERC) under the European Union's Horizon 2020 research and innovation programme (Grant agreement No. 819819) and from the Marie Skłodowska-Curie project PAINLESS under the European Union's Horizon 2020 research and innovation programme (Grant agreement No. 812991). This work was also co-funded by the European Regional Development Fund and the Republic of Cyprus through the Research and Innovation Foundation, under the project INFRASTRUCTURES/1216/0017 (IRIDA).

the UEs employ either the TS, the PS or the AS schemes to decode information and harvest energy simultaneously, while a linear MMSE receiver is equipped for ID and a non-linear EH model is considered. By using stochastic geometry tools, we establish a tractable framework to evaluate several key performance metrics, e.g. coverage probability, average spectral efficiency and average harvested energy, where the analytical expressions for these metrics are derived and several closed-form expressions are obtained for the interference-limited scenarios. Our results show that the MMSE receiver offers a better SWIPT performance compared to conventional MRC. Moreover, it is demonstrated that the PS scheme outperforms the TS and AS in terms of SWIPT performance, by using a MMSE receiver.

Notation: $\Gamma(\cdot)$ and $\Gamma(\cdot,\cdot)$ denote the upper and the lower incomplete Gamma functions, respectively; ${}_2F_1(\cdot,\cdot;\cdot;\cdot)$ is the Gauss hypergeometric function; $(\cdot)^H$ denotes the transpose conjugate; $(n)!$ denotes the factorial of n; $\mathcal{CN}(0,\sigma^2\mathbf{I}_L)$ denotes the circularly symmetric complex Gaussian distribution with zero mean and covariance $\sigma^2\mathbf{I}_L$, $\mathbf{I}_L$ is a $L\times L$ identity matrix; $\mathbb{C}^{1\times L}$ denotes the vector of complex numbers of size L; and $\mathcal{G}(a,b)$ denotes the Gamma distribution with a shape and a scale parameter a and b, respectively.

II. System model

A. Network Model

We consider a two-dimensional cellular network, where the base stations (BSs) are distributed according to a homogeneous Poisson point process (PPP) $\Phi=\{x_i\in\mathbb{R}^2\}$, $i\geq 0$, with density λ, where x_i represents the location of the i-th BS. Moreover, we assume that the UEs are uniformly distributed with a density $\lambda_u\gg\lambda$. Based on the Slivnyak's theorem, we perform our analysis for the typical UE located at the origin, while results hold for any UE in the network [10]. We assume that the typical UE communicates with the closest BS, i.e. the serving BS at x_0.

B. Channel Model

We consider a single-input-multiple-output (SIMO) setup, where all BSs transmit unit-power signals with single omnidirectional antenna, while all UEs are equipped with L antenna elements [6]–[9]. All wireless links are assumed to experience both small-scale fading and large-scale path-loss effect. Specifically, we assume that the small-scale fading coefficients follow a Rayleigh distribution. Thus, the channels between each antenna element of the typical UE and the i-th BS are denoted as $\mathbf{h}_i=[h_{1,i},h_{2,i},\cdots,h_{L,i}]^T$, where $h_{j,i}$ for $i\geq 0$ and $1\leq j\leq L$, are independent and identically distributed (i.i.d.) complex Gaussian random variables with zero mean and unit variance. Regarding the large-scale path loss between a transmitter at X and a receiver at Y, we adopt an unbounded singular path loss model, i.e. $L(X,Y)=\|X-Y\|^{\alpha}$, where $\alpha>2$ is the path loss exponent. Hence, the baseband equivalent received signal at the typical UE can be expressed as

$$\mathbf{y}=r_0^{-\alpha/2}\mathbf{h}_0 s_0+\sum\nolimits_{x_i\in\Phi\setminus x_0} r_i^{-\alpha/2}\mathbf{h}_i s_i+\mathbf{n},$$

where s_0 and s_i are the received signals from the serving and the i-th interfering BSs, respectively, and $\mathbf{n}\in\mathbb{C}^{1\times L}$ represents additive white Gaussian noise, which is distributed based on $\mathcal{CN}(0,\sigma^2\mathbf{I}_L)$.

C. Joint wireless information and power transfer model

We assume that all UEs are able to decode information and harvest energy simultaneously by using the SWIPT technology, based on either the TS, PS or AS schemes. In particular, by adopting the TS scheme, a UE allocates a fraction $\tau\in[0,1]$ of the time slot for ID, while it harvests energy for the remaining time slot. Regarding the scenario where a UE employs the PS scheme, the received RF signal power at each antenna is split into two parts with a ratio $\rho\in[0,1]$, where a fraction ρ of the signal power is allocated for ID and the other is directed to the rectenna for EH. Finally, for the scenario where a UE employs the AS scheme, ℓ antennas are used for ID, where $0\leq\ell\leq L$, and the remaining $L-\ell$ antennas are used for EH [2], [3].

A linear MMSE receiver is assumed to be equipped at each UE, where an optimal weight vector is determined, such that the output SINR is maximized [8], [9]. Hence, the output SINR can be expressed as [9]

$$\gamma=\rho r_0^{-\alpha}\widehat{\mathbf{h}}_0^H\mathbf{R}^{-1}\widehat{\mathbf{h}}_0, \tag{1}$$

with $\mathbf{R}=\sum_{x_i\in\Phi\setminus x_0}\rho r_i^{\alpha}\widehat{\mathbf{h}}_i\widehat{\mathbf{h}}_i^H+\sigma^2\mathrm{I}_\ell$, where $\widehat{\mathbf{h}}_i\subseteq\mathbf{h}_i$ is a ℓ dimensional vector representing the channel coefficients of the links between the i-th BS and the UE's antennas allocated for ID. Note that (1) holds for the TS, PS and AS schemes, i.e.

- $\ell=L$, $\rho=1$ and $0\leq\tau\leq 1$ for the TS scheme,
- $\ell=L$, $\tau=1$ and $0\leq\rho\leq 1$ for the PS scheme,
- $\rho=1$, $\tau=1$ and $0\leq\ell\leq L$ for the AS scheme.

Regarding the energy transfer model, we adopt a practical EH model, which captures the randomness in the detection of the actual harvested energy [11]. More specifically, the harvested energy of a UE is quantified as following [12]

$$\psi=\frac{\bar{\tau}\bar{\rho}\nu\eta}{1+F}\sum\nolimits_{x_i\in\Phi}\sum\nolimits_{j=\ell+1}^{L}|h_{ij}|^2 r_i^{-\alpha},$$

where $\bar{\tau}=1-\tau$ and $\bar{\rho}=1-\rho$, F is an exponential random variable[1] with mean ζ, $\nu=(\zeta e^{\zeta}\int_{-\zeta}^{\infty}e^{-t}/t\mathrm{d}t)^{-1}$ and η is a constant representing the energy conversion efficiency from RF to direct current power.

III. SWIPT performance with a MMSE receiver

We investigate the ID and EH performance for scenarios with a MMSE receiver in terms of several key performance metrics, e.g. ID and EH coverage probabilities, average spectral efficiency and average harvested energy. We analytically derive the exact expressions for the aforementioned performance metrics, by using stochastic geometry tools. Moreover, closed-form expressions of the coverage probabilities are derived for the interference-limited regime.

[1]Such coefficient in the energy transfer phase is used to capture the random noise in the detection and conversion of the actual harvested energy [12].

A. Information transfer performance

We first investigate the ID coverage probability, which is defined as the probability that the output SINR of the MMSE receiver is greater than the decoding threshold β, i.e. $\Pi^{\mathrm{ID}}(\beta) = \mathbb{P}[\gamma \geq \beta]$. The achieved ID coverage probability of the typical UE that employs either the PS or AS scheme[2] is characterized in the following theorem.

Theorem 1. *The ID coverage probability for a MMSE receiver is given by*

$$\Pi^{\mathrm{ID}}(\beta) = \int_0^\infty \frac{\Gamma\left(\ell, \sigma^2\rho^{-1}\beta r^\alpha + \lambda\delta(r,\beta)\right)}{\Gamma\left(\ell\right)} f(r)\mathrm{d}r, \quad (2)$$

where $\delta(r,\beta) = \frac{2\pi r^2 \beta {}_2F_1\left(1, \frac{\alpha-2}{\alpha}; 2-\frac{2}{\alpha}; -\beta\right)}{\alpha-2}$*, and* $f(r)$ *is the probability density function (pdf) of the distance from the typical UE to its serving BS, which is given by [10]*

$$f(r) = 2\pi\lambda r \exp(-\pi\lambda r^2). \quad (3)$$

Proof. See Appendix A. □

Even though the expression in Theorem 1 can be evaluated by using numerical tools, intuitions on how key system parameters affect the ID coverage probability are difficult to derive. Hence, we further simply the expression for ID coverage probability by considering two special cases in the following propositions.

Proposition 1. *By ignoring the noise (i.e. interference-limited regime), the ID coverage probability for a MMSE receiver is given by*

$$\Pi^{\mathrm{ID}}(\beta) = 1 - \left(\frac{\alpha-2}{2\beta {}_2F_1\left(1, \frac{\alpha-2}{\alpha}; 2-\frac{2}{\alpha}; -\beta\right)} + 1\right)^{-\ell}. \quad (4)$$

Proof. See Appendix B. □

From expression (4), we can observe that the density of the BSs, i.e. λ, has no effect on the ID coverage probability of a MMSE receiver, for the interference-limited scenario. This can be indicated by the scale invariance property of the PPP [10]. Moreover, the ID coverage probability depends on the decoding threshold and the number of antennas that are assigned for ID, i.e. β and ℓ, respectively. For a given decoding threshold β, as the number of antennas increases, the ID coverage probability approaches one, i.e. $\lim_{\ell\to\infty} \Pi^{\mathrm{ID}}(\beta) = 1$.

Proposition 2. *For the interference-limited scenario with a propagation exponent* $\alpha = 4$*, the ID coverage probability for a MMSE receiver can be further simplified as*

$$\Pi^{\mathrm{ID}}(\beta) = 1 - \left(\frac{1}{\left(\sqrt{\beta}\arctan(\sqrt{\beta})\right)^{-1} + 1}\right)^{\ell},$$

where $\arctan(\cdot)$ *is the inverse tangent function.*

Note that the ID coverage probability only provides the statistics of the instantaneous SINR observed at the typical UE. Hence, in order to show the achievable data rate, we further investigate the average spectral efficiency. Specifically, the average spectral efficiency is defined as the ergodic Shannon rate per unit bandwidth, i.e. $\eta_{\mathrm{SE}} = \mathbb{E}[\tau\log(1+\gamma)]$, which is evaluated in the following proposition [13].

Proposition 3. *The average spectral efficiency achieved by a MMSE receiver is given by*

$$\eta_{\mathrm{SE}} = \tau\int_0^\infty \frac{\Pi^{\mathrm{ID}}(\beta)}{\beta+1}\mathrm{d}\beta. \quad (5)$$

Proof. The proof is directly from the definition of the ergodic Shannon rate and the average spectral efficiency [13]. □

B. Energy transfer performance

We investigate the EH performance in terms of the EH coverage probability and the average harvested energy. Specifically, the EH coverage probability is defined as the probability that the instantaneous harvested energy is higher than the EH threshold ϵ, i.e. $\Pi^{\mathrm{EH}}(\epsilon) = \mathbb{P}[\psi \geq \epsilon]$. The following theorem provides a closed-form expression for the EH coverage probability.

Theorem 2. *The EH coverage probability of the typical UE is given by*

$$\Pi^{\mathrm{EH}}(\epsilon) = 1 - \exp\left(\zeta + 2\pi\lambda\frac{\Gamma\left(-\frac{2}{\alpha}\right)s^{2/\alpha}\Gamma\left(L-\ell+\frac{2}{\alpha}\right)}{\alpha\Gamma(L-\ell)}\right), \quad (6)$$

where $s = \frac{\bar{\tau}\bar{\rho}\nu\eta\zeta}{\epsilon}$.

Proof. See Appendix C. □

From the expression in Theorem 2, we can observe that, if the number of antennas used for EH purpose becomes large (i.e., $L-\ell\to\infty$), the EH coverage probability approaches one, i.e. $\lim_{L-\ell\to\infty}\Pi^{\mathrm{EH}}(\epsilon) = 1$. Furthermore, a denser deployment of the BSs can improve EH performance. Specifically, in the ultra-dense networks with infinite BSs' density, the EH coverage probability is equal to one, i.e. $\lim_{\lambda\to\infty}\Pi^{\mathrm{EH}}(\epsilon) = 1$.

Proposition 4. *For the special case with* $\alpha = 4$*, the EH coverage probability of the typical UE can be further simplified as*

$$\Pi^{\mathrm{EH}}(\epsilon) = 1 - \exp\left(\zeta - \frac{\pi^2\lambda\sqrt{s}\big(2(L-\ell)\big)!}{4^{L-\ell}(L-\ell-1)!(L-\ell)!}\right).$$

Proof. Based on the expression given in Theorem 2 and the resulting expression $\Gamma\left(\frac{1}{2}+n\right) = \frac{(2n)!}{4^n n!}\sqrt{\pi}$, the simplified expression for the EH coverage probability can be obtained. □

We further assess the EH performance in terms of the average harvested energy, which is defined as the average amount of energy harvested by the typical UE per unit time. The analytical expression of the average harvested energy is provided in the following theorem.

Theorem 3. *The average harvested energy of the typical UE is given by*

$$\bar{\psi} = \frac{2\pi\lambda\bar{\tau}\bar{\rho}(L-\ell)\eta r_m^{2-\alpha}}{\alpha-2}, \quad (7)$$

[2]Note that the TS ratio, i.e. τ, has no effect on the ID coverage probability and thus is not considered.

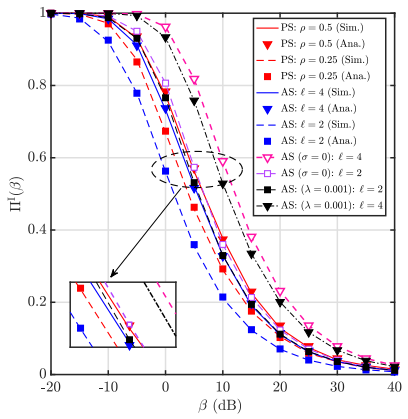

Fig. 1: ID coverage probability versus the ID threshold (β), for the considered PS and AS schemes, where $\rho \in \{0.5, 0.25\}$ and $\ell \in \{4, 2\}$.

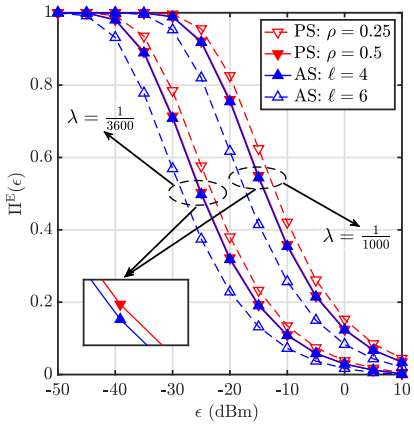

Fig. 2: EH coverage probability versus the EH threshold for the considered PS and AS schemes, where $\rho \in \{0.5, 0.25\}$ and $\ell \in \{4, 6\}$.

where r_m represents the minimum propagation distance between the typical UE and BSs.

Proof. See Appendix D. □

IV. Numerical Results

We provide both simulation and theoretical results to validate the accuracy of our model, and to illustrate the performance and potential benefits of the considered system model. Unless otherwise stated, in our results we use the following parameters: $\lambda = 1/3600$, $\alpha = 4$, $L = 8$, $\zeta = 0.01$, $\eta = 0.7$, $r_m = 1$, $\beta = 10$ dB, $\epsilon = -30$ dBm and $\sigma^2 = -60$ dB.

Fig. 1 shows the ID coverage probability achieved by a MMSE receiver under the PS and AS schemes. In particular, Fig. 1 plots the ID coverage probability versus the decoding threshold for different AS and PS partitioning parameters, i.e. $\ell \in \{2, 4\}$ and $\rho \in \{0.25, 0.5\}$, respectively. Firstly, we can observe that a higher ID coverage probability is achieved with a larger number of antennas or a larger power splitting ratio. This is based on the fact that, for the AS scheme, by allocating more antennas for ID, the output SINR of the MMSE receiver is enhanced; while for the PS scheme, by allocating more received signal power for ID, the effects of noise are suppressed accordingly, thereby resulting in a higher SINR. We can also observe that, with denser network deployments ($\lambda = 0.001$), the interference limited scenario provides a tight approximation with the exact ID coverage probability. Finally, the agreement between the theoretical results (markers) and the simulation results (solid and dash curves) validates our mathematical analysis.

Fig. 2 illustrates the impact of the AS and the PS schemes on the EH coverage probability for different densities of the BSs, i.e. $\lambda \in \{1/3600, 1/1000\}$. Firstly, we can observe that a denser deployment of BSs achieves a higher EH coverage probability. This is based on the fact that, a denser network provides more multi-user interference, which can be used for EH. Moreover, it can be observed that by allocating more antennas or more signal power for EH purpose, the EH performance is improved. It is also indicated that for the case where the half received power or half number of antennas are allocated for EH based on the PS and AS scheme, respectively, the PS scheme achieves a slightly higher EH coverage probability than the AS scheme. Based on the results in Theorem 2, TS scheme achieves the identical EH coverage probability with PS scheme for a same splitting ratio. Hence, due to the space limitation, only PS and AS schemes are presented in Fig. 2.

Fig. 3 depicts the ID and EH coverage probability regions achieved by MRC and MMSE receivers, with different number of receiving antennas $L \in \{4, 8, 16\}$, where the AS scheme is employed and the noise power is ignored. We can observe a clear trade-off between the ID and the EH performance for any number of receiving antennas. This was expected since, by allocating more number of antennas for ID (or EH) purpose, the corresponding performance is improved, while on the other hand, the EH (or ID) coverage probability is decreased since less resources are allocated. Similarly, by increasing the total number of antennas, both the ID and the EH performance is improved. Moreover, Fig. 3 plots the performance achieved by the MRC receiver for comparison purpose [6]. We can observe that, the MMSE outperforms the MRC for any number of antennas. This is based on the fact that the MMSE receiver is an optimal combining approach, which yields a maximum output SINR, while the MRC receiver is a low-complexity approach and achieves a worse performance when the interference signals are correlated.

Fig. 4 reveals the impact of different SWIPT schemes on the average spectral efficiency and harvested energy. Specifically, Fig. 4 plots the average spectral efficiency and average harvested energy regions for TS, PS and AS schemes achieved by the MMSE receiver. We can observe from the figure that PS scheme offers the best SWIPT performance. This observation is in line with the results presented in Fig. 1 & 2. More specifically, PS and TS schemes result in a similar ID coverage

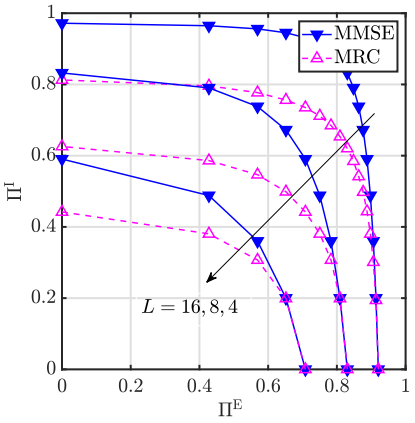

Fig. 3: ID and EH coverage probability regions for the MMSE and MRC receivers, where $L = \{16, 8, 4\}$, $\beta = 10$ dB and $\epsilon = -30$ dBm.

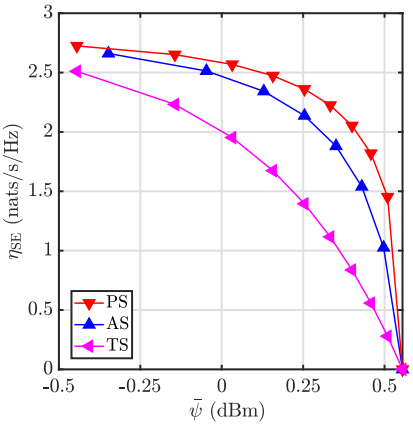

Fig. 4: Average spectral efficiency and average harvested energy regions for the MMSE receiver, where $L = 8$, $\sigma^2 = -60$ dB and $\lambda = \frac{1}{3600}$.

probability (slightly outperform the AS scheme), while PS schemes offers more time for ID compared to TS scheme, hence achieving a higher spectral efficiency. In addition, based on the expression 7, for any same splitting ratio of the TS, PS and AS schemes, i.e. $\bar{\tau} = \bar{\rho} = \frac{L-\ell}{L}$, the achieved average harvested energy are equal. Hence, the best SWIPT performance is achieved by the PS scheme for the MMSE receiver.

V. Conclusion

In this paper, we investigated the SWIPT technology in the terms of a linear MMSE receiver. By leveraging stochastic geometry tools, we established a tractable mathematical framework to evaluate the SWIPT performance for multiple antennas UEs. Based on TS, PS or AS schemes, exact analytical expressions for the ID and EH coverage probabilities, average spectral efficiency and average harvested energy were derived, while simple closed-form expressions were obtained for the interference-limited case. Our results have shown that, the MMSE receiver outperforms the conventional MRC in terms of SWIPT performance. We have also revealed that the PS scheme offers a better SWIPT performance compared to the TS and AS schemes by using a linear MMSE receiver.

Appendix A
Proof of Theorem 1

Firstly, by conditioning on the distance from the typical UE to BSs, the conditional ID coverage probability is given by [8]

$$\mathbb{P}[\gamma \geq \beta | r_0, r_1, \ldots, r_K] = \frac{\exp\left(-\sigma^2 \beta r_0^{\alpha}\right) \sum_{i=0}^{\ell-1} a_i (\beta r_0)^i}{\prod_{j=1}^{K} \left(1 + r_j^{-\alpha} \beta r_0\right)},$$

where K is the number of BSs, $r_i = \|x_i\|$ represents the distance from the typical UE to i-th BS, and a_i are the first ℓ coefficient of the Taylor expansion of $\exp\left(-\sigma^2 \beta r_0^{\alpha}\right) \prod_{j=1}^{N} (1 + r_j^{-\alpha} \beta r_0)$.

Then, by un-conditioning over the distance from the typical UE to interfering BSs, i.e. $r_1, r_2, \cdots, r_K$, and following [9, Eq.(15)], the conditional ID coverage probability, i.e. $\mathbb{P}[\gamma \geq \beta | r_0]$ can be expressed as

$$\begin{aligned}\mathbb{P}[\gamma \geq \beta | r_0] = &\exp\left(-\frac{\sigma^2 \beta r_0^{\alpha}}{\rho}\right) \sum_{j=0}^{\ell-1} \sum_{k=0}^{j} \frac{(\sigma^2 \rho^{-1} \beta r_0^{\alpha})^{j-k}}{k!(j-k)!} \\ &\times \left(2\pi\lambda \int_{r_0}^{\infty} \frac{x^{1-\alpha} \beta r_0^{\alpha}}{1 + x^{-\alpha} \beta r_0^{\alpha}} \mathrm{d}x\right)^k \\ &\times \exp\left(-2\pi\lambda \int_{r_0}^{\infty} \frac{x^{1-\alpha} \beta r_0^{\alpha}}{1 + x^{-\alpha} \beta r_0^{\alpha}} \mathrm{d}x\right).\end{aligned}$$

The above integrals can be evaluated, by using the transformation $u \leftarrow x^2$ and by using the expression in [14, 3.24], such that we have

$$\begin{aligned}\mathbb{P}[\gamma \geq \beta | r_0] = &\exp\left(-\frac{\sigma^2 \beta r_0^{\alpha}}{\rho}\right) \sum_{j=0}^{\ell-1} \sum_{k=0}^{j} \frac{(\sigma^2 \rho^{-1} \beta r_0^{\alpha})^{j-k}}{k!(j-k)!} \\ &\times \big(\lambda \delta(r_0, \beta)\big)^k \exp\big(-\lambda \delta(r_0, \beta)\big),\end{aligned}$$

where $\delta(r_0, \beta) = \frac{2\pi r_0^2 \beta_2 F_1\left(1, \frac{\alpha-2}{\alpha}; 2 - \frac{2}{\alpha}; -\beta\right)}{\alpha - 2}$. Then, by using the binomial theorem [15], the above expression can be further reconstructed as

$$\begin{aligned}\mathbb{P}[\gamma \geq \beta | r_0] = &\exp\left(-\frac{\rho \lambda \delta(r_0, \beta) + \beta r_0^{\alpha} \sigma^2}{\rho}\right) \\ &\times \sum_{j=0}^{\ell-1} \frac{(\sigma^2 \rho^{-1} \beta r_0^{\alpha} + \lambda \delta(r_0, \beta))^j}{j!} \\ = &\frac{\Gamma\left(\ell, \sigma^2 \rho^{-1} \beta r_0^{\alpha} + \lambda \delta(r_0, \beta)\right)}{\Gamma(\ell)},\end{aligned}$$

where the final step is based on the expression in [16, Eq(8.69)]. Finally, by un-conditioning with respect to r_0, the result in Theorem 1 can be obtained.

APPENDIX B
PROOF OF PROPOSITION 1

For the interference-limited scenario the additive noise is neglected, and hence the ID coverage probability can be simplified by utilizing the transformation $x \leftarrow \delta(r_0, \beta)$, which yields

$$\Pi^{\mathrm{I}}(\beta) = \int_0^{\infty} \frac{\Gamma(\ell, x)}{\Gamma(\ell)} \exp\left(-\frac{x(\alpha-2)}{2\beta y}\right) \frac{\alpha-2}{2\beta y} \mathrm{d}x,$$

where $y = {}_2F_1\left(1, \frac{\alpha-2}{\alpha}; 2-\frac{2}{\alpha}; -\beta\right)$. Then, by using the resulting expression [14, 6.451], the desired expression is obtained.

APPENDIX C
PROOF OF THEOREM 2

We re-write the EH coverage probability as

$$\mathbb{P}[\psi \geq \epsilon] = \mathbb{P}\left[F \leq \frac{\bar{\tau}\bar{\rho}\nu\eta}{\epsilon} \sum\nolimits_{x_i \in \Phi} \sum\nolimits_{j=\ell+1}^{L} |h_{j,i}|^2 r_i^{-\alpha} - 1\right],$$

Since F is an exponential random variable with mean ζ, the above equation can be expressed as

$$\mathbb{P}[\psi \geq \epsilon] = 1 - \mathbb{E}\left[\prod\nolimits_{x_i \in \Phi} \exp\left(-\frac{\bar{\tau}\bar{\rho}\nu\eta\zeta c_i}{\epsilon r_i^{\alpha}}\right)\right] \exp(\zeta), \quad (8)$$

where $c_i = \sum_{j=\ell+1}^{L} |h_{j,i}|^2$. Since for the Rayleigh fading, the channel power gain is an exponential random variable, i.e. $|h_{j,i}|^2 \sim \exp(1)$, c_i is a Gamma distributed random variable with shape parameter $L-\ell$ and unit scale, i.e. $c_i \sim \mathcal{G}(L-\ell, 1)$ [6]. Therefore, the above expectations can be evaluated as following

$$\begin{aligned}
&\mathbb{E}\left[\prod\nolimits_{x_i \in \Phi} \int_0^{\infty} \exp\left(-\frac{\bar{\tau}\bar{\rho}\nu\eta\zeta c}{\epsilon r_i^{\alpha}}\right) \frac{\exp(-c) c^{L-\ell-1}}{\Gamma(L-\ell)} \mathrm{d}c\right] \\
&\overset{(a)}{=} \mathbb{E}\left[\prod\nolimits_{x_i \in \Phi} \left(\frac{\epsilon r_i^{\alpha}}{\bar{\tau}\bar{\rho}\nu\eta\zeta + \epsilon r_i^{\alpha}}\right)^{L-\ell}\right] \\
&\overset{(b)}{=} \exp\left(-2\pi\lambda \int_0^{\infty} \left(1 - \left(\frac{\epsilon r^{\alpha}}{\bar{\tau}\bar{\rho}\nu\eta\zeta + \epsilon r^{\alpha}}\right)^{L-\ell}\right) r \mathrm{d}r\right), \quad (9)
\end{aligned}$$

where (a) is derived based on the resulting expression [14, 3.351] and (b) follows from the probability generating functional of a PPP [10]. Finally, by evaluating the above integral and by substituting (9) into (8), the final result in Theorem 2 is derived.

APPENDIX D
PROOF OF THEOREM 3

The average harvested energy is evaluated by averaging the instantaneous harvested energy over the random channel and path loss components, i.e.

$$\begin{aligned}
\bar{\psi} =& \mathbb{E}\left[\frac{\bar{\tau}\bar{\rho}\nu\eta}{1+F} \sum\nolimits_{x_i \in \Phi} \sum\nolimits_{j=\ell+1}^{L} |h_{ij}|^2 r_i^{-\alpha}\right] \\
=& \underbrace{\mathbb{E}\left[\frac{\nu}{1+F}\right]}_{=1} \mathbb{E}\left[\bar{\tau}\bar{\rho}\eta \sum\nolimits_{x_i \in \Phi} \sum\nolimits_{j=\ell+1}^{L} |h_{ij}|^2 r_i^{-\alpha}\right] \\
\overset{(a)}{=}& \mathbb{E}\left[\bar{\tau}\bar{\rho}\eta(L-\ell) \sum\nolimits_{x_i \in \Phi} r_i^{-\alpha}\right] \\
=& \bar{\tau}\bar{\rho}\eta(L-\ell) \int_{r_m}^{\infty} 2\pi\lambda r^{1-\alpha} \mathrm{d}r,
\end{aligned}$$

where (a) follows from the fact that the channel power gain $|h_{i,j}|^2$ are i.i.d. exponential random variable with mean one [10]. Finally, by evaluating the above integral, the final results are derived.

REFERENCES

[1] T. Huang, W. Yang, J. Wu, J. Ma, X. Zhang, and D. Zhang, "A survey on green 6G network: Architecture and technologies," *IEEE Access*, vol. 7, pp. 175 758–175 768, Dec. 2019.

[2] I. Krikidis, S. Timotheou, S. Nikolaou, G. Zheng, D. W. K. Ng, and R. Schober, "Simultaneous wireless information and power transfer in modern communication systems," *IEEE Commun. Mag.*, vol. 52, no. 11, pp. 104–110, Nov. 2014.

[3] R. Zhang and C. K. Ho, "MIMO broadcasting for simultaneous wireless information and power transfer," *IEEE Trans. Wireless Commun.*, vol. 12, no. 5, pp. 1989–2001, May 2013.

[4] M. Di Renzo and W. Lu, "System-level analysis and optimization of cellular networks with simultaneous wireless information and power transfer: Stochastic geometry modeling," *IEEE Trans. Veh. Technol.*, vol. 66, no. 3, pp. 2251–2275, Mar. 2017.

[5] Q. Wu and R. Zhang, "Weighted sum power maximization for intelligent reflecting surface aided SWIPT," *IEEE Commun. Lett.*, vol. 9, no. 5, pp. 586–590, May 2020.

[6] R. Tanbourgi, H. S. Dhillon, J. G. Andrews, and F. K. Jondral, "Effect of spatial interference correlation on the performance of maximum ratio combining," *IEEE Trans. Commun.*, vol. 13, no. 6, pp. 3307–3316, Jun. 2014.

[7] Y. Wang, F. Liu, C. Wang, P. Wang, and Y. Ji, "Outage probability of SIMO MRC receivers with correlated poisson field of interferers," *IEEE Commun. Lett.*, vol. 25, no. 1, pp. 74–78, Jan. 2021.

[8] H. Gao, P. Smith, and M. Clark, "Theoretical reliability of MMSE linear diversity combining in Rayleigh-fading additive interference channels," *IEEE Trans. Commun.*, vol. 46, no. 5, pp. 666–672, May 1998.

[9] O. B. S. Ali, C. Cardinal, and F. Gagnon, "Performance of optimum combining in a Poisson field of interferers and Rayleigh fading channels," *IEEE Trans. Wireless Commun.*, vol. 9, no. 8, pp. 2461–2467, Aug. 2010.

[10] M. Haenggi, *Stochastic Geometry for Wireless Networks.* Cambridge University Press, 2012.

[11] X. Lu, I. Flint, D. Niyato, N. Privault, and P. Wang, "Self-sustainable communications with RF energy harvesting: Ginibre point process modeling and analysis," *IEEE J. Sel. Areas Commun.*, vol. 34, no. 5, pp. 1518–1535, Apr. 2016.

[12] N. Deng and M. Haenggi, "The energy and rate meta distributions in wirelessly powered D2D networks," *IEEE J. Sel. Areas Commun.*, vol. 37, no. 2, pp. 269–282, Sep. 2019.

[13] S. S. Kalamkar, F. Baccelli, F. M. Abinader, A. S. M. Fani, and L. G. U. Garcia, "Beam management in 5G: A stochastic geometry analysis," *IEEE Trans. Wireless Commun.*, vol. 21, no. 4, pp. 2275–2290, Sep. 2022.

[14] I. S. Gradshteyn and I. M. Ryzhik, *Table of integrals, series, and products*. Elsevier, 2007.

[15] G. Upton and I. Cook, *A Dictionary of Statistics*. OUP Oxford, 2008.

[16] G. B. Arfken and H. J. Weber, *Mathematical methods for physicists*, 6th ed. Elsevier, 2005.